

Submicron three-dimensional infrared GaAs/Al_xO_y-based photonic crystal using single-step epitaxial growth

Jayshri Sabarinathan, Pallab Bhattacharya,^{a)} Donghai Zhu, Boaz Kochman, Weidong Zhou, and Pei-Chen Yu

Solid State Electronic Laboratory, Department of Electrical Engineering and Computer Science, University of Michigan, Ann Arbor, Michigan 48109-2122

(Received 1 February 2001; accepted for publication 21 March 2001)

A relatively simple technique is demonstrated to fabricate three-dimensional face-centered-cubic infrared photonic crystals with submicron feature sizes using GaAs-based technology, single-step epitaxial growth, and lateral wet oxidation. The photonic crystals were fabricated with feature sizes (a) of 1.5 and 0.5 μm . Transmission measurements reveal a stopband centered at 1.0 μm with a maximum attenuation of 10 dB for the submicron ($a=0.5 \mu\text{m}$) photonic crystal. This technique is scalable to small photonic crystal periodicity and hence to shorter wavelengths. © 2001 American Institute of Physics. [DOI: 10.1063/1.1372198]

It has been shown that certain three-dimensional (3D) photonic crystals exhibit complete band gaps where electromagnetic waves cannot propagate in any direction. Since the first proposal of these photonic materials by Yablonovitch¹ and by John,² photonic band gaps (PBGs) have been realized and observed at microwave and optical frequencies in a variety of macroscopic and microscopic materials. Different techniques to fabricate 3D photonic crystals in GaAs and silicon-based material systems have been reported.^{3–15} Layer-by-layer fabrication of diamond-like structures in GaAs- (Ref. 9) and Si-based¹⁰ materials at optical wavelengths have been achieved. Single-step deposition processes in Si-based systems have also been achieved.¹¹ However these techniques reported so far involve either repetitive alignment and processing steps which are cumbersome or Si-based or are not scalable to submicron feature sizes, rendering them difficult to integrate with existing active optoelectronic devices.

We describe here a simple fabrication scheme to produce a face-centered-cubic (fcc) photonic crystal, shown schematically in Fig. 1(a) with submicron feature sizes using single-step epitaxial growth and GaAs-based technology. The technique is scalable to submicron dimensions and will allow integration of the photonic crystal with other active optoelectronic devices or passive optical components made with similar semiconductors. As far as the authors are aware, this is the first demonstration of a single-step process to fabricate submicron GaAs-based 3D fcc photonic crystals. Transmission measurements were performed on the photonic crystals fabricated to determine the transmission characteristics.

The starting point in the fabrication of the photonic crystal is the definition of a checkerboard pattern on a (001) GaAs substrate. Depending on the periodicity desired, optical or electron-beam lithography is used. A 200 Å Ti/550 Å Ni bilayer is deposited on e-beam patterned resist and subsequently the checkerboard pattern is transferred to the metal layer by a lift-off process. With the Ti/Ni acting as the etch

mask, a combination of wet and dry reactive ion etching (RIE) is used to transfer the pattern to the GaAs substrate to a depth of 0.25 μm . The metal mask is next removed and the patterned wafer, shown in the inset of Fig. 1(b), is cleaned and inserted into a molecular beam epitaxy (MBE) growth system. After oxide desorption, four periods of alternating 0.2 μm Al_{0.98}Ga_{0.02}As/0.2 μm Al_{0.30}Ga_{0.70}As are deposited. The Al_{0.98}Ga_{0.02}As layers will provide the low index dielectric regions (after subsequent oxidation), while the Al_{0.30}Ga_{0.70}As layers will provide the high index dielectric regions of the photonic crystal. The choice of 30% Al in the high index layers is to facilitate the epitaxial process as ex-

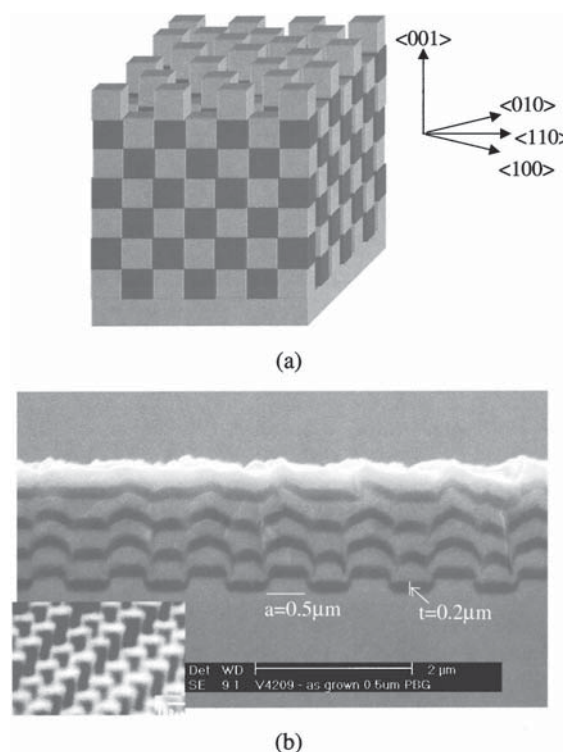


FIG. 1. (a) Schematic of a 3D fcc photonic band gap crystal; (b) SEM image of the cross section of a tetragonal fcc PBG crystal with feature size $a = 0.5 \mu\text{m}$ and $t = 0.2 \mu\text{m}$ after MBE growth of four periods, with the inset depicting the SEM image of a (001) patterned GaAs substrate.

^{a)}Electronic mail: pkb@eecs.umich.edu

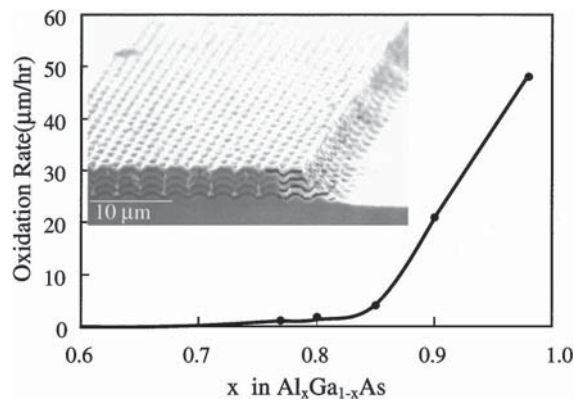


FIG. 2. Oxidation rate of $\text{Al}_x\text{Ga}_{1-x}\text{As}$ as a function of Al composition at 450°C , with the inset depicting the SEM image of the cross section of the photonic band gap crystal after ridge etch and wet oxidation.

plained in the next paragraph. The samples after MBE growth, shown in Fig. 1(b), are taken out of the MBE chamber and ridges $30\ \mu\text{m}$ wide and $4\ \mu\text{m}$ high are formed by optical lithography and wet etching. The ridges are necessary to expose the layers for the selective lateral wet oxidation process. These samples are inserted into an open tube quartz furnace and lateral wet oxidation is performed at 450°C for 20 min in an ambient of flowing N_2 (75 sccm) saturated with water vapor by bubbling it through a H_2O bath held at 95°C . The $\text{Al}_{0.98}\text{Ga}_{0.02}\text{As}$ layers are preferentially oxidized to form stable Al_xO_y . We have thus created a 3D photonic crystal in a fcc lattice, schematically shown in Fig. 1(a), in which lattice site regions of refractive index ~ 3.55 are embedded in an Al_xO_y matrix of refractive index 1.5. The index contrast is therefore ~ 2 .

A scanning electron microscope (SEM) image of the cross sections of the PBG crystal after growth and wet oxidation is shown in the inset of Fig. 2. There are several aspects of this simple process that need to be highlighted and discussed. First, the realization of an ideal fcc structure requires MBE growth of the right thickness to occur in the grooves and mesa tops. However, such growth will cause discontinuities in the layer structures wherein the $\text{Al}_{0.98}\text{Ga}_{0.02}\text{As}$ layer cannot be wet oxidized. We found that by etching $\{111\}$ facets on the corners of the patterned mesas, a more conformal growth of the layers is obtained, thus providing a continuous path in both $\langle 001 \rangle$ directions. This allows the lateral wet oxidation of the $\text{Al}_{0.98}\text{Ga}_{0.02}\text{As}$ layers to occur. The result is a modified fcc structure. Second, the success of the technique crucially depends on the growth kinetics of the adatoms on the patterned substrate. When the feature sizes become comparable to the migration length of the adatoms, preferential growth occurs at the edges of the mesas and grooves, which act as kink sites for adatom incorporation. This leads to a nonplanar surface and the initial pattern is lost within a couple of periods. The migration of Ga adatoms is $\sim 1\ \mu\text{m}$ at 560°C .¹⁶ The migration of Al adatoms is much less. By decreasing the growth temperature to 450°C and by adding a small amount of Al to the GaAs layer, the migration length can be decreased considerably, allowing conformal growth of the layers for feature sizes $< 1\ \mu\text{m}$. However, it is not desirable to increase the Al content in the high index layer by too much because the wet oxidation rate of this layer has to be maintained as almost negligible to

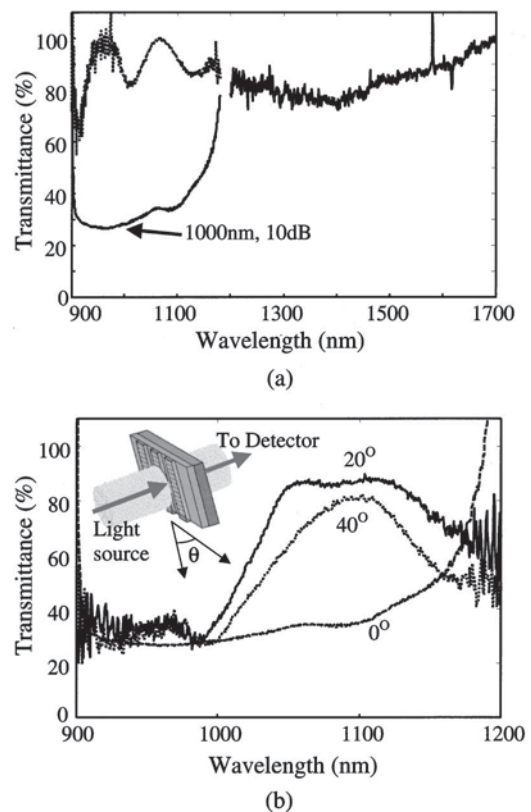


FIG. 3. Surface normal transmission characteristics of a 3D PBG structure with (a) feature size of $a = 0.5\ \mu\text{m}$ and $t = 0.2\ \mu\text{m}$ for four periods. A transmittance dip centered at a wavelength of $1\ \mu\text{m}$ is observed. The spectra from 900 to 1200 and 1200 to 1700 nm are taken with a PMT and a Ge detector, respectively. The dotted line represents the control structure transmission spectrum. (b) Angular dependence of the measured transmittance for different angles (0° – 40°) from the surface normal.

provide oxidation selectivity.^{17,18} The wet oxidation rate of $\text{Al}_x\text{Ga}_{1-x}\text{As}$ as a function of composition x is shown in Fig. 2. We found the ideal situation is to use $\text{Al}_{0.30}\text{Ga}_{0.70}\text{As}$ instead of GaAs as the high index material. The growth rate is $\sim 2\ \text{\AA/s}$. The $\text{Al}_{0.98}\text{Ga}_{0.02}\text{As}$ layers were grown at 580°C . Therefore a growth interruption was necessary after the growth of this layer to reduce the substrate temperature to 450°C . It was found that the insertion of a $30\ \text{\AA}$ GaAs layer provided good protection to the $\text{Al}_{0.98}\text{Ga}_{0.02}\text{As}$ layer during the interruption.

The transmission spectrum of the submicron photonic crystal was measured at room temperature using a white light source, a monochromator, liquid nitrogen-cooled photomultiplier tube (PMT), and Ge detector in the wavelength range of 900–1700 nm. The measurement results for light incident in the surface normal direction on the PBG structure with $0.5\ \mu\text{m}$ feature size (a) are shown in Fig. 3(a). The samples were thinned down to $< 70\ \mu\text{m}$ and polished. The spectrum was normalized by the measured spectra of the GaAs substrate. A transmittance dip centered at $1\ \mu\text{m}$ with a maximum attenuation of $\sim 10\ \text{dB}$ is seen. The gap is in the expected wavelength range. Also shown is the normalized transmission spectrum of an unpatterned multilayer control sample which shows a negligible transmission dip over the measured wavelength range as compared with the photonic crystal sample. The angular dependence of the transmission spectrum of the photonic crystal was also investigated. Measurements were

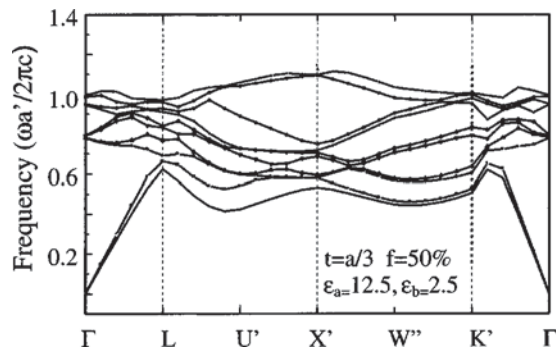


FIG. 4. Calculated band structure for a tetragonal fcc PBG crystal with feature size $a = 0.5 \mu\text{m}$ and $t = 0.2 \mu\text{m}$ showing a gap at the X' point (surface normal) between 0.8 and 1.1 (normalized frequency) corresponding to a wavelength range of $1.24\text{--}0.9 \mu\text{m}$. Note that a' corresponds to a $2\times$ feature size (a).

made at angles θ ($0 \leq \theta \leq 40^\circ$) to the normal as shown in Fig. 3(b). This corresponds to a change in incident beam direction from $\Gamma\text{--}X'$ towards $\Gamma\text{--}K'$ of the tetragonal face-centered-cubic PBG crystal. We observe that the transmission gap decreases in width as the sample is rotated. Theoretical calculations, using the plane-wave expansion technique,¹⁹ were also done for a tetragonal fcc structure with feature size of $a = 0.5 \mu\text{m}$ and $t = 0.2 \mu\text{m}$ thick layers (in the z direction). The calculated band structure is shown in Fig. 4. We can see that it shows a gap for k around the X' direction (surface normal) between 0.9 and $1.24 \mu\text{m}$ (corresponding to a normalized frequency of $1.1\text{--}0.8$) which agrees very well with the measured transmission results. One interesting feature that we consistently observe in the transmission spectra of the PBG structures of all periodicities is the existence of a double dip in the measured stopbands. The transmission data on GaAs-based photonic crystals from other research groups^{9,12} show similar characteristics. It

could be due to the fringe effects introduced by the multilayer $\text{Al}_{0.98}\text{Ga}_{0.02}\text{As}/\text{Al}_{0.30}\text{Ga}_{0.70}\text{As}$ structure or a feature of the photonic crystal band structure.

This work was supported by the Defense Advanced Research Projects Agency under Grant No. MDA 972-00-1-0020.

¹E. Yablonovitch, J. Opt. Soc. Am. B **10**, 283 (1993).

²S. John, Phys. Rev. Lett. **58**, 2486 (1987).

³S. Fan, P. R. Villeneuve, and J. D. Joannopoulos, J. Appl. Phys. **78**, 1415 (1995).

⁴J. D. Joannopoulos, P. R. Villeneuve, and S. Fan, Nature (London) **386**, 143 (1997).

⁵S. Y. Lin, J. G. Fleming, D. L. Hetherington, B. K. Smith, R. Biswas, K. M. Ho, M. Sigalas, W. Zubrzycki, S. R. Kurtz, and J. Bur, Nature (London) **394**, 251 (1998).

⁶S. Y. Lin, and J. G. Fleming, J. Lightwave Technol. **17**, 1944 (1999).

⁷K. M. Ho, C. T. Chan, C. M. Soukoulis, R. Biswas, and M. Sigalas, Solid State Commun. **89**, 413 (1994).

⁸H. S. Sözüer and J. W. Haus, J. Opt. Soc. Am. B **10**, 296 (1993).

⁹S. Noda, N. Yamamoto, M. Imada, H. Kobayashi, and M. Okano, J. Lightwave Technol. **17**, 1948 (1999).

¹⁰P. Bhattacharya, W. Zhou, D. Zhu, and J. Sabarinathan, Appl. Phys. Lett. **75**, 1670 (1999).

¹¹S. Kawakami, Electron. Lett. **33**, 1260 (1997).

¹²L. Zavieh and T. S. Mayer, Appl. Phys. Lett. **75**, 2533 (1999).

¹³C. Cuisin, A. Chelnokov, J. Lourtioz, D. Decanini, and Y. Chen, Appl. Phys. Lett. **77**, 770 (2000).

¹⁴R. De La Rue, Phys. Vibrations **6**, 229 (1998).

¹⁵S. Romanov, H. Yates, M. Pemble, and R. De La Rue, J. Phys.: Condens. Matter **12**, 8221 (2000).

¹⁶M. Hata, T. Isu, A. Watanabe, and Y. Katayama, Appl. Phys. Lett. **56**, 2542 (1990).

¹⁷H. Gebretsadik, Ph.D. thesis, University of Michigan, Ann Arbor, MI, 1999.

¹⁸K. Choquette, K. Geib, C. Ashby, R. Twisten, O. Blum, H. Hou, D. Follstaedt, B. Hammons, D. Mathes, and R. Hull, IEEE J. Sel. Top. Quantum Electron. **3**, 916 (1997).

¹⁹R. D. Meade, A. M. Rappe, K. D. Brommer, and J. D. Joannopoulos, Phys. Rev. **48**, 8434 (1993).